

On the use and significance of isentropic potential vorticity maps

By B. J. HOSKINS¹, M. E. MCINTYRE² and A. W. ROBERTSON³

¹ Department of Meteorology, University of Reading

² Department of Applied Mathematics and Theoretical Physics, University of Cambridge

³ Laboratoire de Physique et Chimie Marines, Université Pierre et Marie Curie, 75230 Paris Cedex 05

(Received 12 February 1985, revised 2 July 1985)

SUMMARY

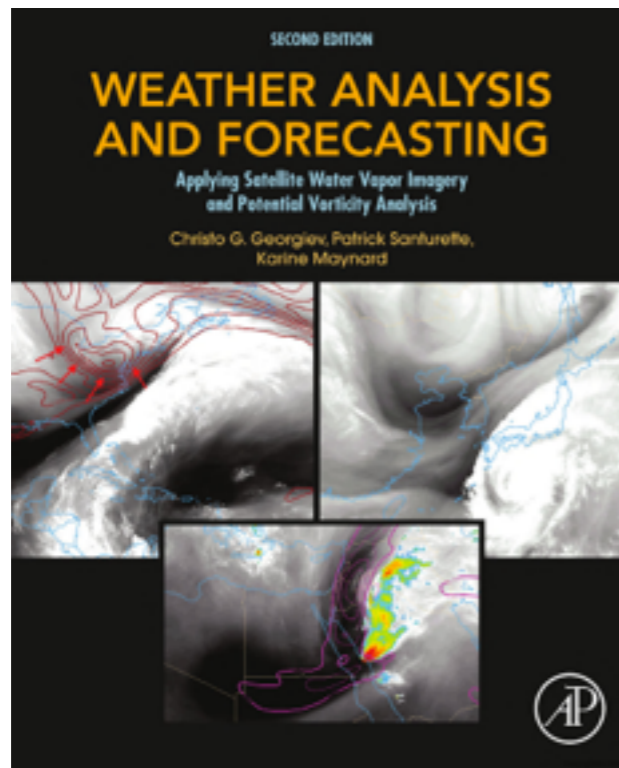
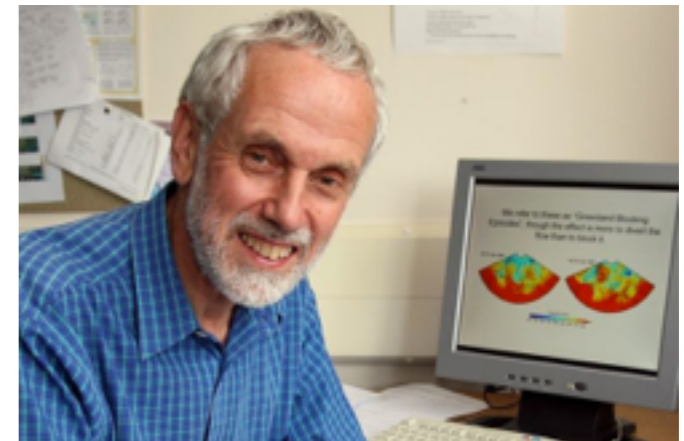
The two main principles underlying the use of isentropic maps of potential vorticity to represent dynamical processes in the atmosphere are reviewed, including the extension of those principles to take the lower boundary condition into account. The first is the familiar Lagrangian conservation principle, for potential vorticity (PV) and potential temperature, which holds approximately when advective processes dominate frictional and diabatic ones. The second is the principle of 'invertibility' of the PV distribution, which holds whether or not diabatic and frictional processes are important. The invertibility principle states that if the total mass under each isentropic surface is specified, then a knowledge of the global distribution of PV on each isentropic surface and of potential temperature at the lower boundary (which within certain limitations can be considered to be part of the PV distribution) is sufficient to deduce, diagnostically, all the other dynamical fields, such as winds, temperatures, geopotential heights, static stabilities, and vertical velocities, under a suitable balance condition. The statement that vertical velocities can be deduced is related to the well-known omega equation principle, and depends on having sufficient information about diabatic and frictional processes. Quasi-geostrophic, semi-geostrophic, and 'nonlinear normal mode initialization' realizations of the balance condition are discussed. An important constraint on the mass-weighted integral of PV over a material volume and on its possible diabatic and frictional change is noted.

Some basic examples are given, both from operational weather analyses and from idealized theoretical models, to illustrate the insights that can be gained from this approach and to indicate its relation to classical synoptic and air-mass concepts. Included are discussions of (a) the structure, origin and persistence of cutoff cyclones and blocking anticyclones, (b) the physical mechanisms of Rossby wave propagation, baroclinic instability, and barotropic instability, and (c) the spatially and temporally nonuniform way in which such waves and instabilities may become strongly nonlinear, as in an occluding cyclone or in the formation of an upper air shear line. Connections with principles derived from synoptic experience are indicated, such as the 'PV-A rule' concerning positive vorticity advection on upper air chains, and the role of disturbances of upper air origin, in combination with low-level warm advection, in triggering latent heat release to produce explosive cyclonic development. In all cases it is found that time sequences of isentropic potential vorticity and surface potential temperature charts—which succinctly summarise the combined effects of vorticity advection, thermal advection, and vertical motion without requiring explicit knowledge of the vertical motion field—lead to a very clear and complete picture of the dynamics. This picture is remarkably simple in many cases of real meteorological interest. It involves, in principle, no sacrifices in quantitative accuracy beyond what is inherent in the concept of balance, as used for instance in the initialization of numerical weather forecasts.

“On the use and significance of isentropic potential vorticity maps”

(By B. J. Hoskins, M. E. McIntyre, and A. W. Robertson)

(Professor Sir Brian Hoskins from <http://www.getreading.co.uk/>)

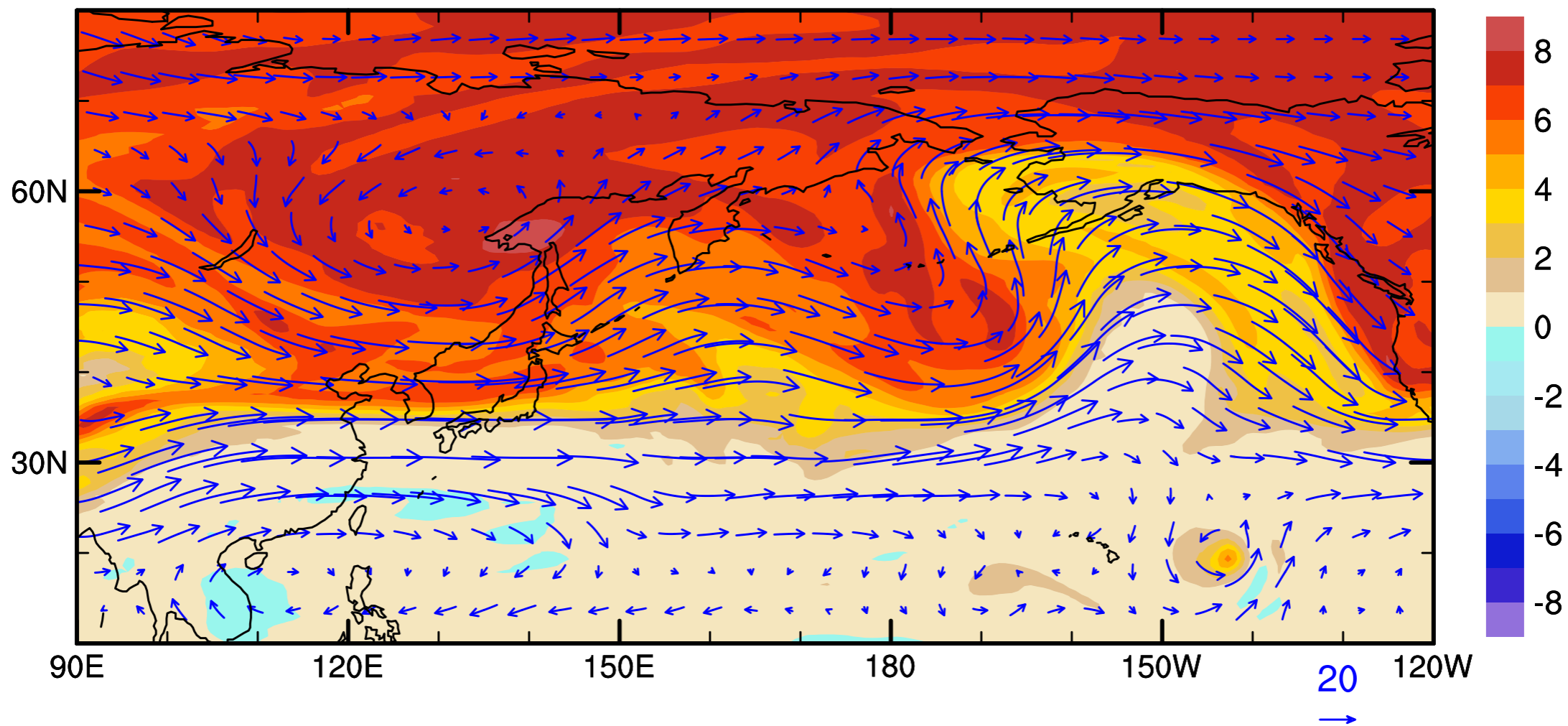


“Weather Analysis and Forecasting: Applying Satellite Water Vapor Imagery and Potential Vorticity Analysis”

(By Christo Georgiev, Patrick Santurette, Karine)

PV(PVU) and wind(m/s) at 330 K

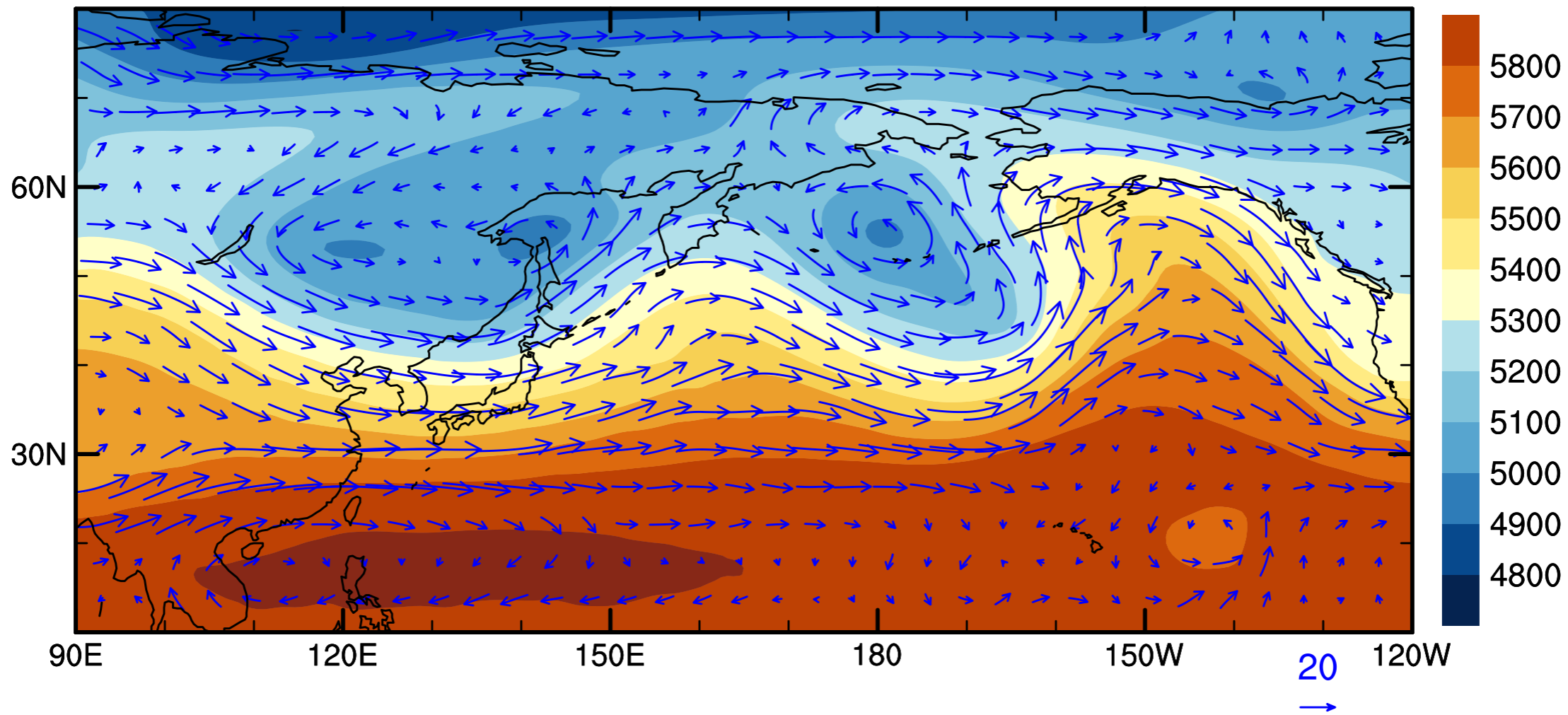
20151225



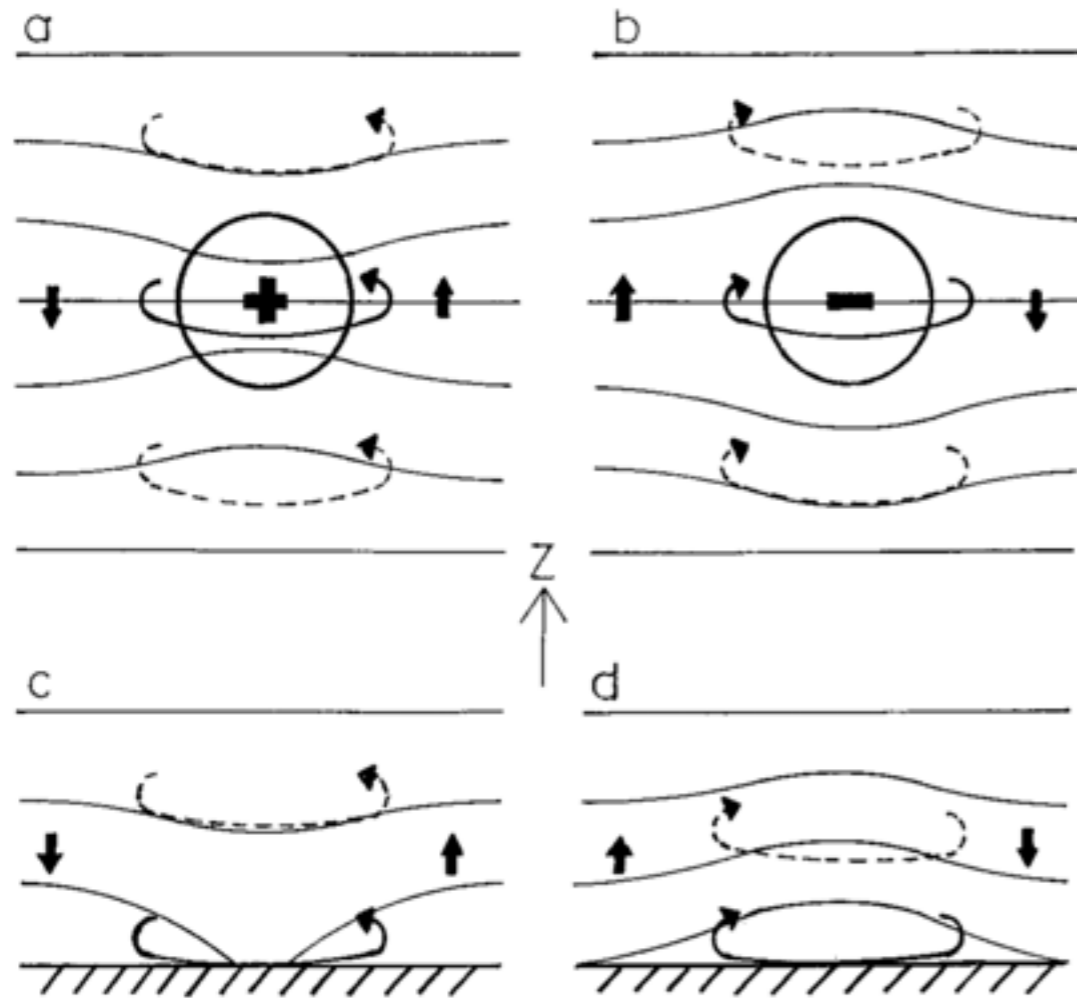
Shading : potential vorticity

GPH(m) and wind(m/s) at 500hPa

20151225



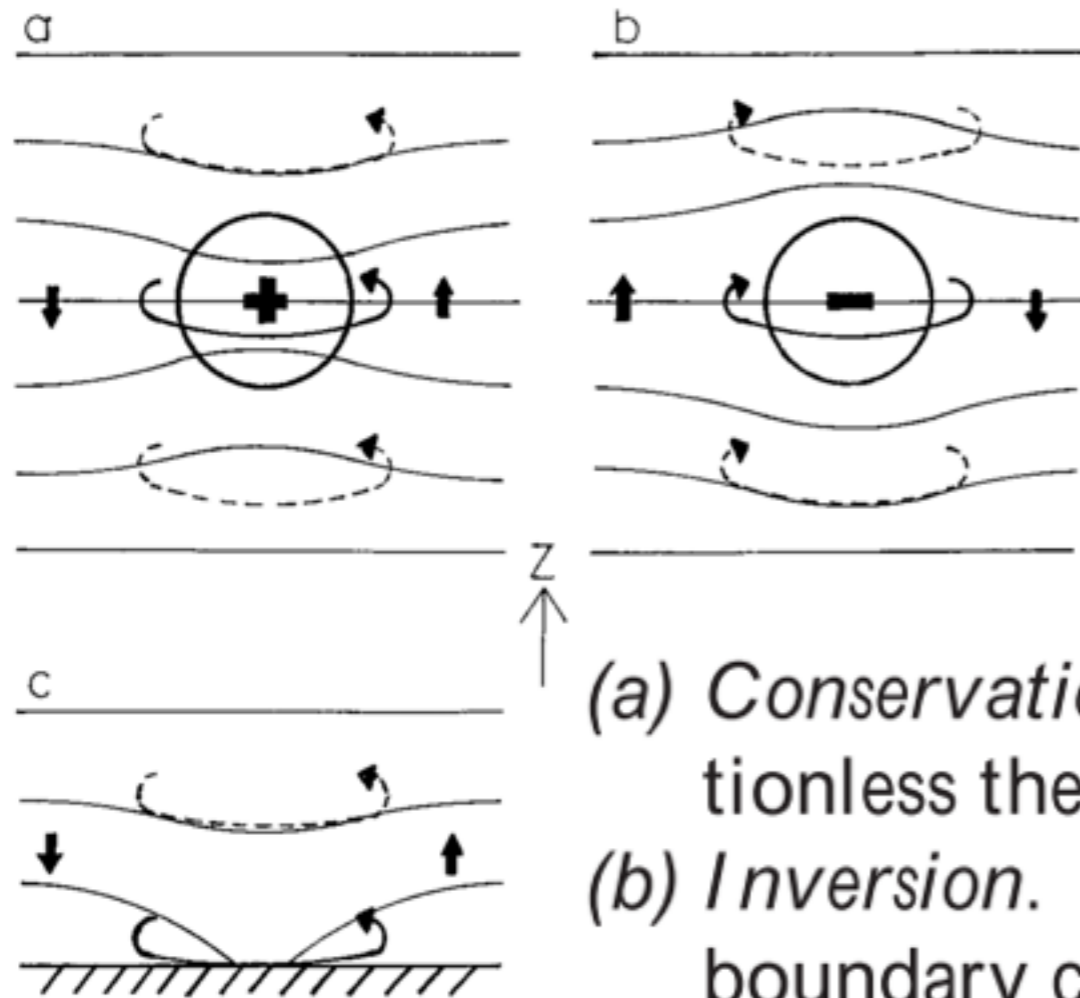
(Rossby-Ertel) Potential Vorticity



$$PV = \frac{\vec{\omega}_a \cdot \nabla \theta}{\rho}$$

(where $\vec{\omega}_a$ = absolute vorticity in 3D)

(Rossby-Ertel) Potential Vorticity



$$PV = \frac{\vec{\omega}_a \cdot \nabla \theta}{\rho}$$

(where $\vec{\omega}_a$ = absolute vorticity in 3D)

- (a) *Conservation.* If the motion is adiabatic and frictionless then PV is conserved moving with the air.
- (b) *Inversion.* Given PV everywhere and suitable boundary conditions, and assuming that the motion is balanced in the sense that it is not composed of fast gravity waves (or acoustic waves), then equations can be solved to obtain ϕ , v , θ , w , etc. This is analogous to the two-dimensional and QGPV cases discussed above. [\(remote response\)](#)

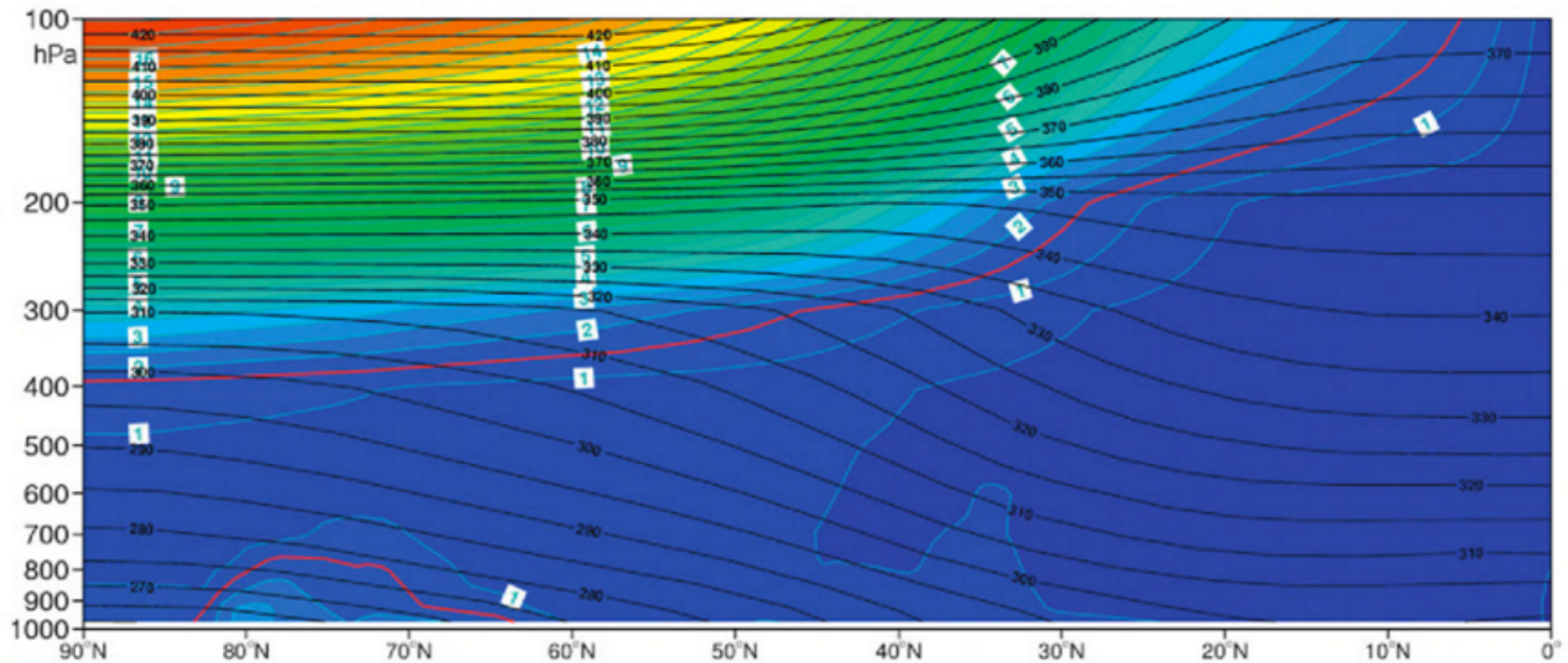


FIGURE 1.4

Zonal year average (vertical cross-section) of the potential vorticity (PV; *color areas*, every 0.5 PVU) and of the potential temperature (*black lines* in K, interval 5K) in the Northern Hemisphere. The contour of PV value = 1.5 PVU (the so-called dynamical tropopause) is given in *red*. This chart used data from 44 years of the European Center for Medium Range Weather Forecasting reanalysis, 1958–2001.

From Malardel (2008).

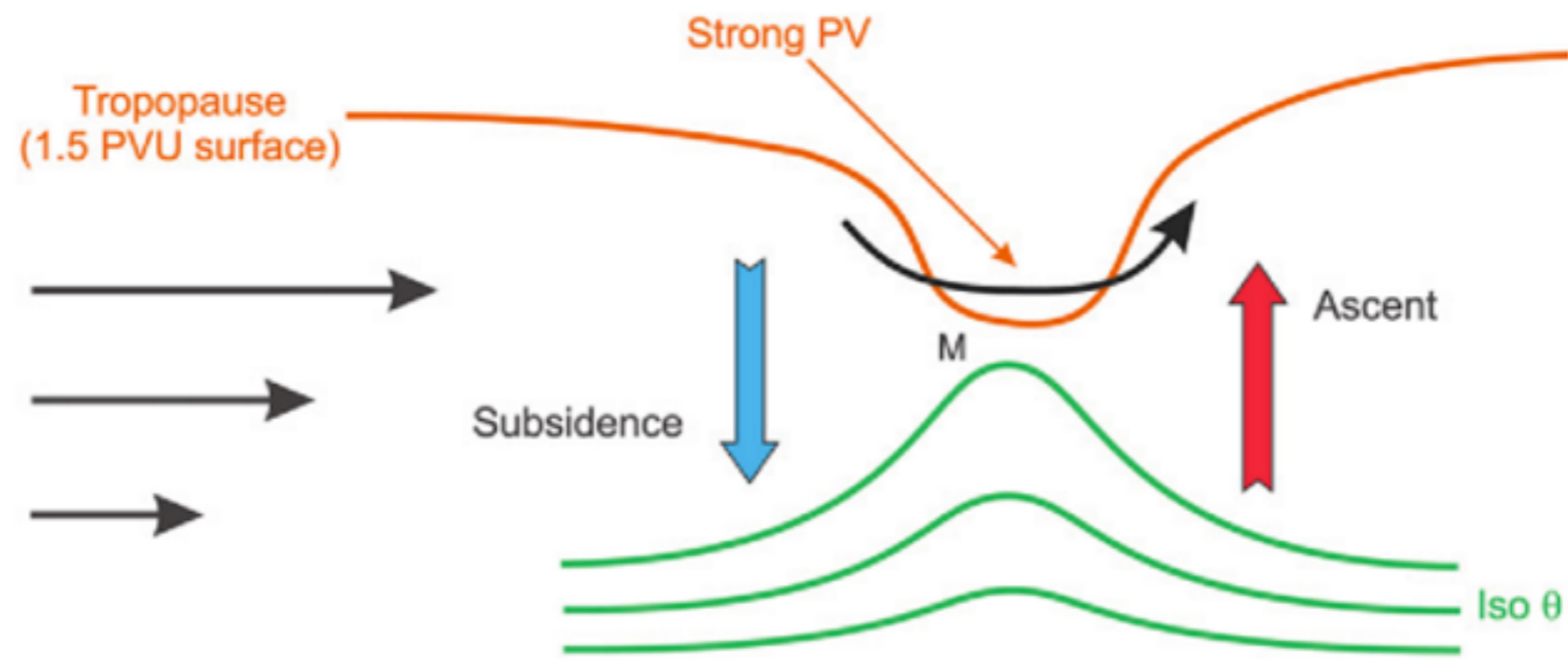


FIGURE 1.7

A schematic cross-section, showing an idealized model of the modification of the troposphere associated with an upper-level positive potential vorticity anomaly, which is referred to as a dynamical tropopause anomaly.

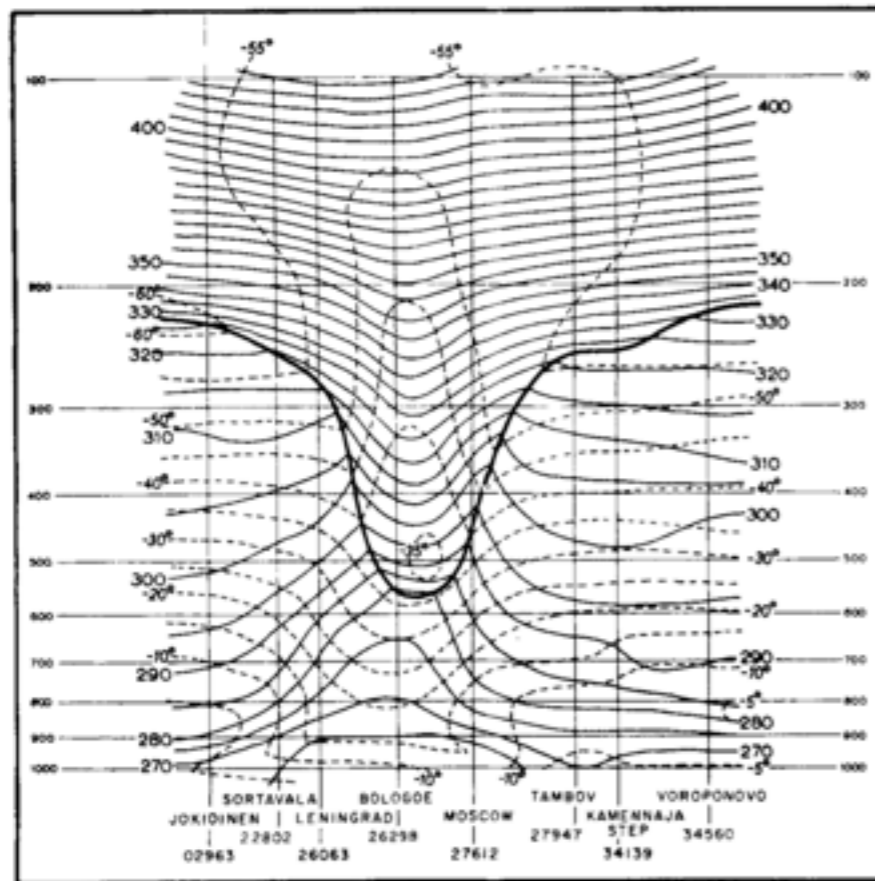
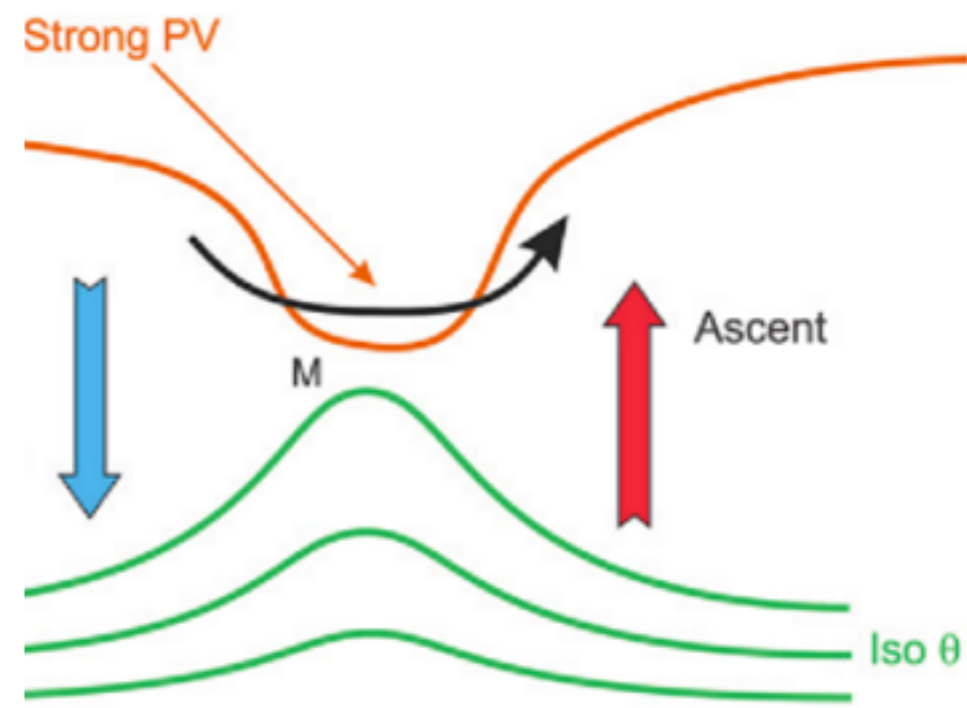


Figure 8. A vertical section through a cutoff cyclone at 12 GCT November 16 1959 produced by Peltonen (1963). The heavy line represents the tropopause; dashed lines are isotherms at 5°C intervals and solid lines isentropes every 5 K. The centre of the cyclone was at about 35°E, 58°N.



odel of the modification of the troposphere associated with which is referred to as a dynamical tropopause anomaly.

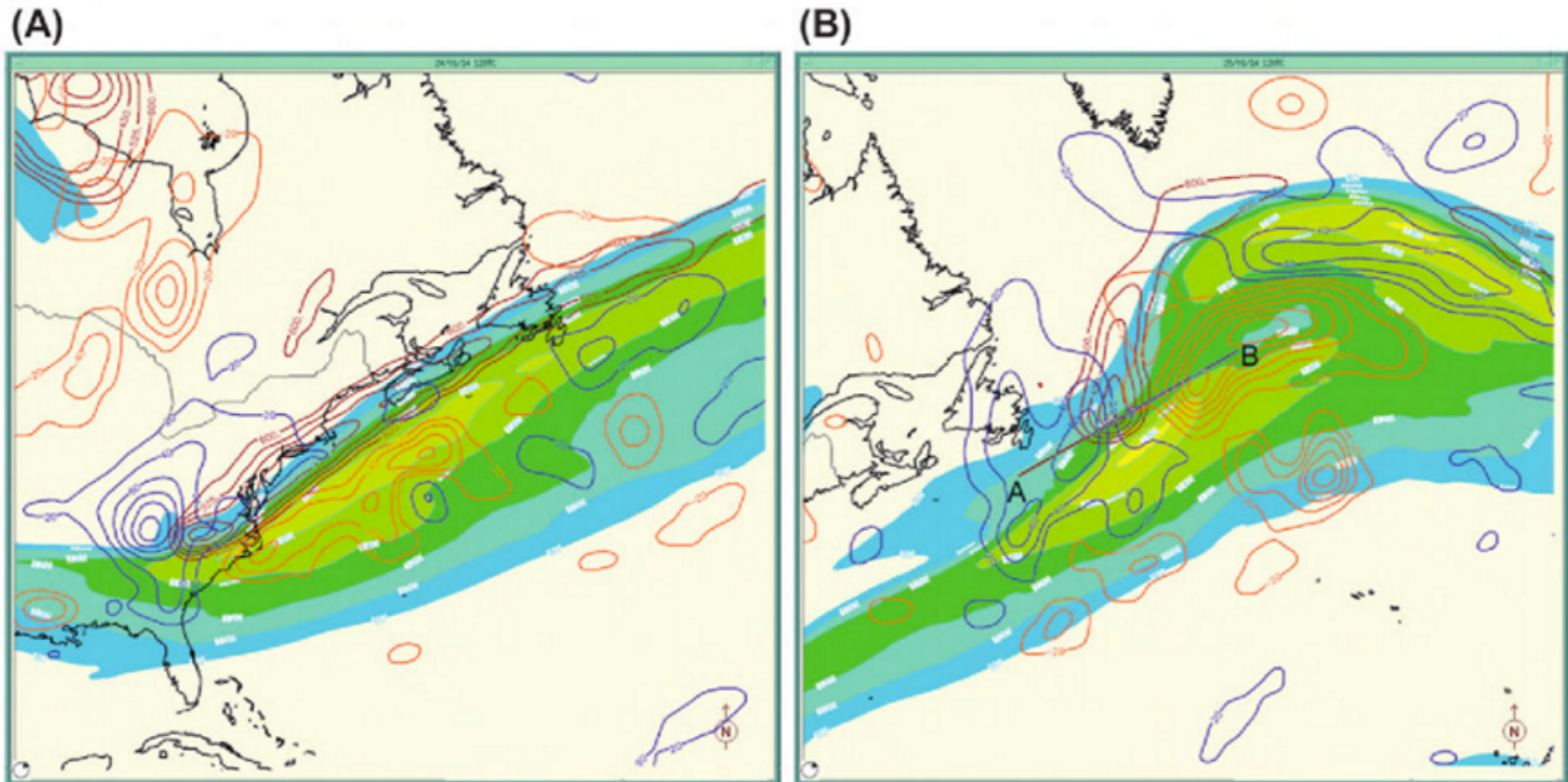


FIGURE 1.11

Isotachs of the wind at 300 hPa greater than 80 kt (*color*, every 20 kt) and vertical velocity at 600 hPa (ascending motion in *orange*, descending motion in *blue*, every $20 \times 10^{-2} \text{ Pa/s}$). ARPEGE model analysis (A) 24 January 2014 1200 UTC, (B) 25 January 2014 1200 UTC. The *black line* in (B) is the axis of the cross-sections presented in Fig. 1.12.

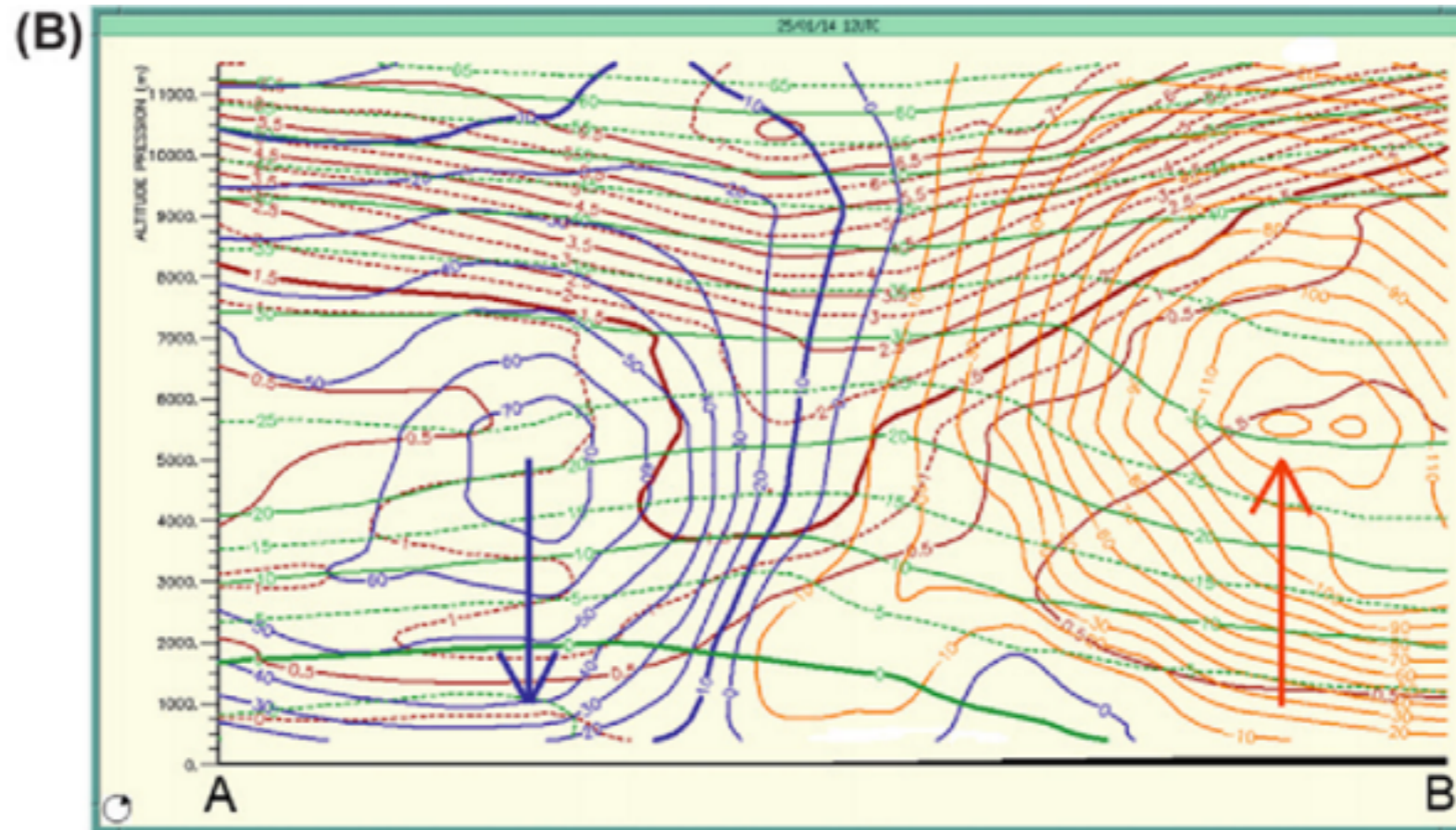
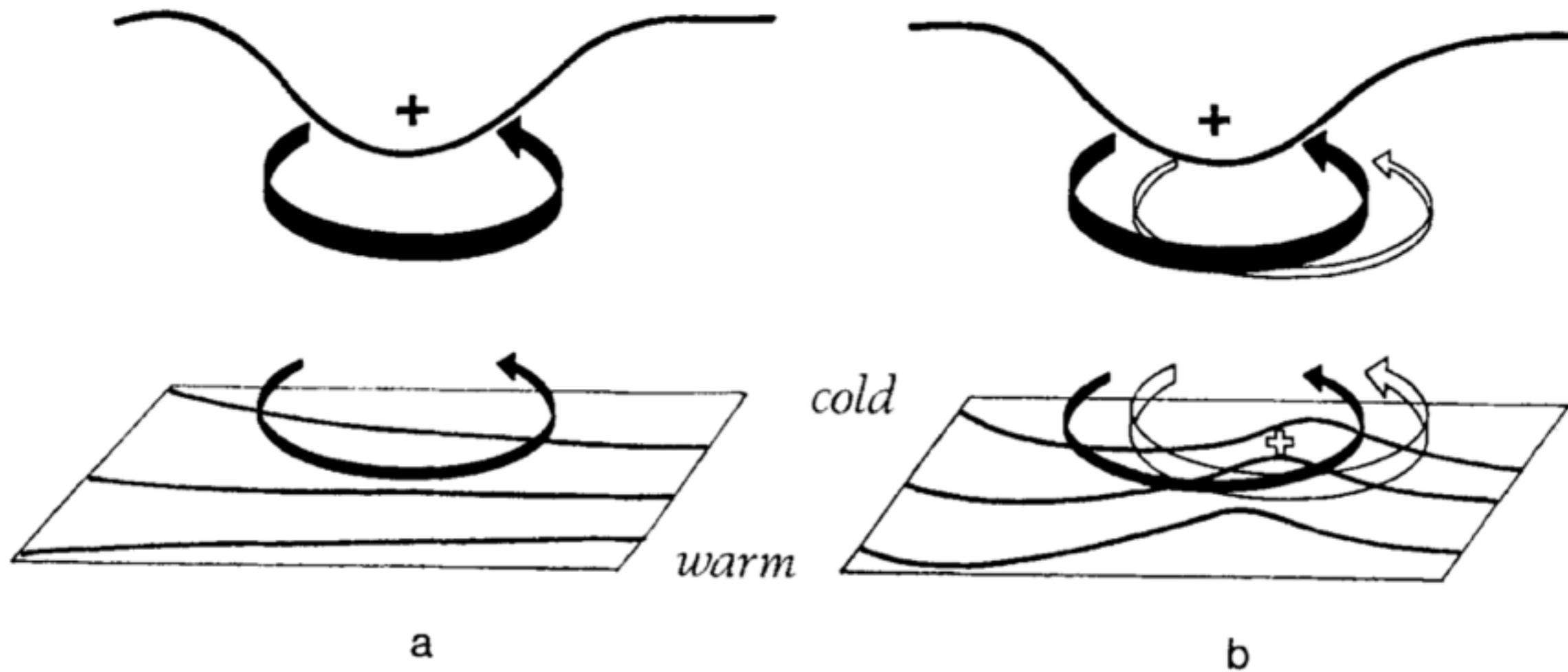
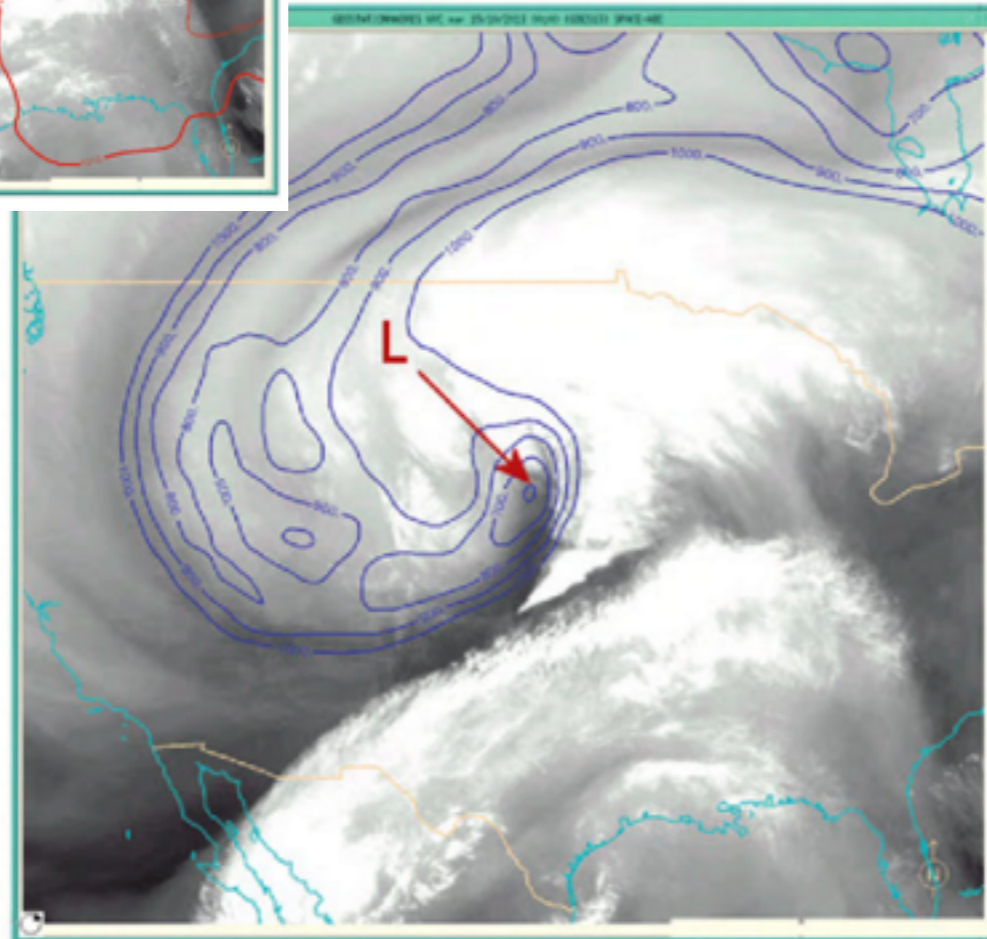
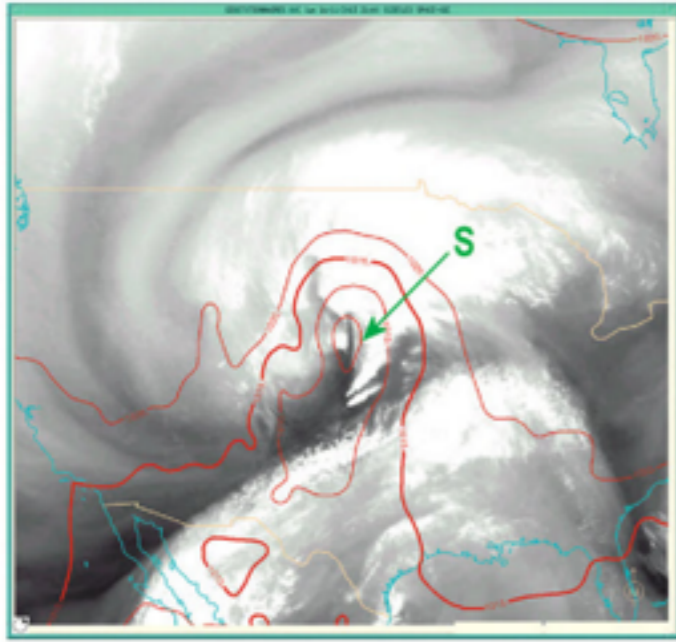


FIGURE 1.12

Vertical cross-section along the southwest–northeast (noted SW NE) axis marked in *black line* in Fig. 1.11B, from ARPEGE model analysis on 25 January 2014 at 1200 UTC. Potential vorticity contours are in *brown* (intervals of 0.5 PVU, 1.5 PVU contour solid); iso- θ surfaces ($^{\circ}\text{C}$) are in *green*. Also shown in (A) the wind component transverse to the plane of the cross-section (in *black*, kt: *solid lines* indicate the wind in the cross-section plane, and the *dashed lines* indicate the wind out of the cross-section plane). Also shown in (B) the ascending (in *orange*) and the descending (in *blue*) motion (10^{-2} Pa/s).



(B)



(D)

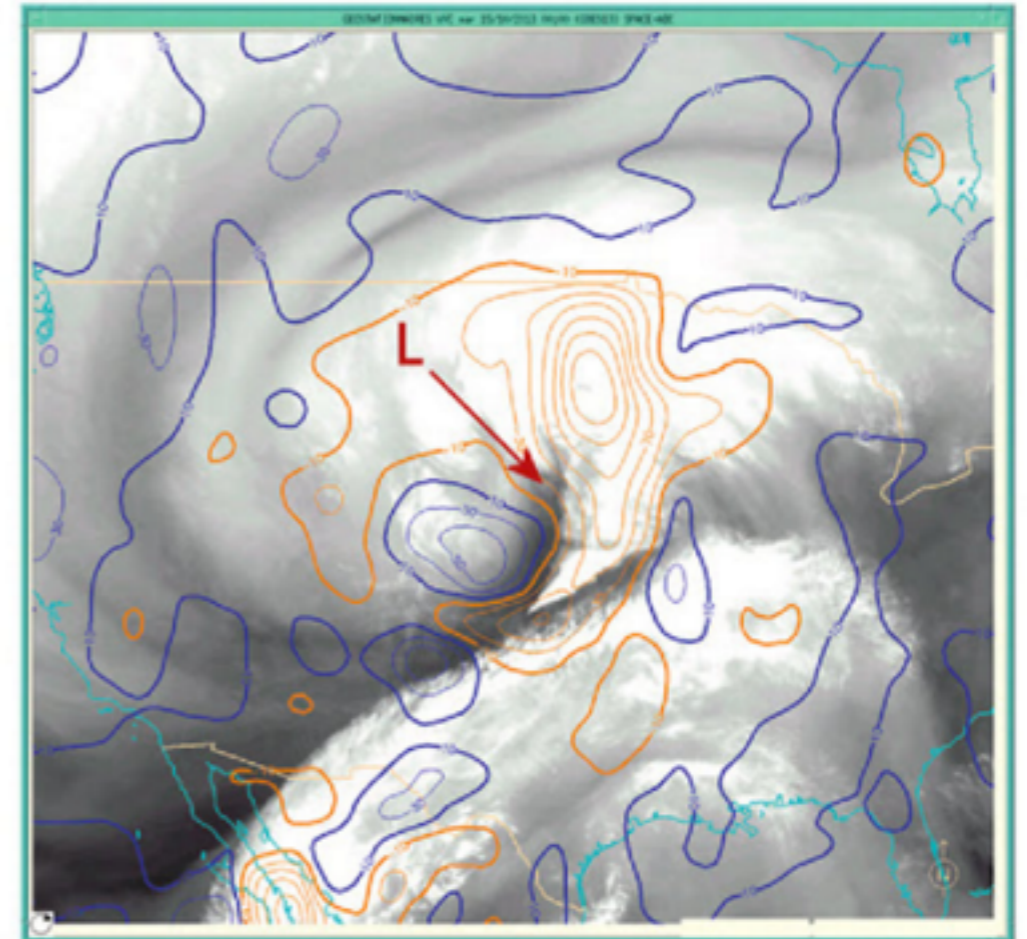


FIGURE 3.5

Dry intrusion over North America as seen in the GOES water vapor images overlaid by ARPEGE analysis fields: for October 14, 2013 of mean sea level pressure (brown, threshold 1020 hPa) (A) at 1800 UTC and (B) at 2100 UTC; for October 15, 2013, 0000 UTC of (C) 1.5 PVU surface heights (dam, blue only ≤ 1000 dam) and (D) vertical motions at 700 hPa (10^{-2} Pa/s, ascending in orange, descending in blue). Also marked: "L," the surface low center.

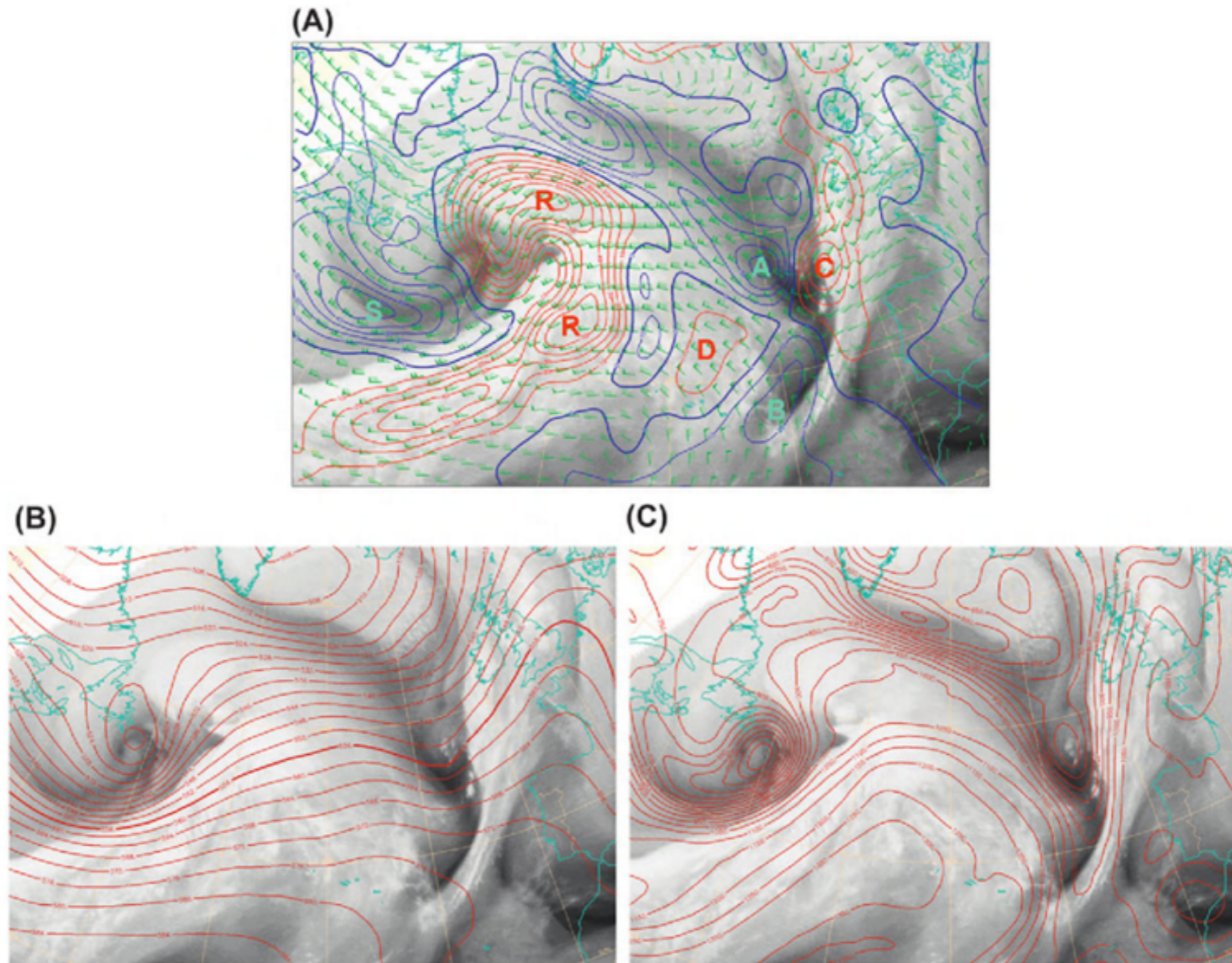


FIGURE 3.1

A water vapor image overlaid by (A) vertical motions (10^{-2} Pa/s, ascending in red, descending in blue) at 400 hPa and wind (*green arrows*) at 300 hPa; (B) 500 hPa heights (dam); (C) geopotential height (dam) of the 1.5 PVU surface.